MAGNETIC AND XPS STUDIES ON RNi_5 (R=La, Nd, Tb, Dy)-BASED COMPOUNDS

E. Burzo[1)], S. Chiuzbaian[2)], L. Chioncel[3)], A. Takacs[1,2)], M. Neumann[2)], I. Creanga[1)]

[1)]Faculty of Physics, Babes-Bolyai University, 400084 Cluj-Napoca, Romania
[2)]Fachbereich Physik, Universitat Osnanbrück, D-49069 Osnanbrück, Germany
[3)]Department of Physics, University of Nijmegen 6500 GL, Nijmegen, The Netherlands

Abstract

Magnetic measurements and XPS studies were performed on $LaNi_{5-x}Al_x$, $TbNi_{5-x}Al_x$, $DyNi_{5-x}Al_x$, $LaNi_{5-x}Cu_x$ and $NdNi_{5-x}Cu_x$ systems. In addition, band structure calculations were also performed. The nickel moments in RNi_5 (R=Nd, Tb, Dy) compounds are of $\cong 0.17\ \mu_B$ and $\cong 0.25\ \mu_B$ at 2c and 3g sites, respectively. The nickel moments, in low temperature range, decrease when increasing Al or Cu content and are practically nil for $x > 1$. The 4f-5d-3d exchange interactions were analyzed and the contributions of local 4f-5d and short range 5d-3d exchange interactions to 5d band polarization are estimated. An effective field of the order of (30-40) T is necessary to induce a nickel moment, at 1.7 K. Above the Curie temperatures, the effective nickel moments were determined. The $LaNi_{5-x}Cu_x$ and $LaNi_{5-x}Al_x$ systems, show, at $T \leq 10$ K, a T^2 dependence of the magnetic susceptibilities, while above a characteristic temperature T^*, a Curie-Weiss contribution was evidenced. The magnetic behaviour of nickel is analyzed in models, which take into account electron correlation effects in d bands.

1. Introduction

The RNi_5 based compounds, where R is a rare-earth or yttrium were intensively studied in correlation with their use as hydrogen storage materials [1]. The RNi_5 compounds crystallize in a hexagonal structure of $CaCu_5$-type, having P6/mmm space group. In this structure the R atoms occupy 1a-type site, while nickel ones are distributed on 2c and 3g positions. The analysis of the magnetic properties of RNi_5 end series compounds evidenced interesting properties. The Curie temperatures, T_c, are very low, the maximum value, $T_c = 35$ K, being reported for $GdNi_5$. In earlier studies it was suggested that nickel is non-magnetic in RNi_5-series. This fact was correlated with the paramagnetic behaviour of $LaNi_5$ and YNi_5 compounds. Later on, analyzing the magnetic properties of $(Gd_xY_{1-x})Ni_5$ [2] and $(Gd_xLa_{1-x})Ni_5$ [3] pseudobinary compounds, it has been shown that the mean magnetic nickel moment, at 1.7 K, in $GdNi_5$ is of $\cong 0.17\ \mu_B$/atom, antiparallel oriented to gadolinium moment. The nickel saturation moments decrease when substituting Gd by La or Y and are nil in $LaNi_5$ and YNi_5. In the RNi_5 (R=La,Y) [4,5], the magnetic susceptibilities, χ, at $T \leq 10$ K follow a T^2 dependence. Above a characteristic temperature, T^*, the χ^{-1} vs T shows a linear dependence as described by the Curie-Weiss law. The magnetic behaviour of these systems was analyzed in the spin fluctuation model [6].

The $RNi_{5-x}Cu_x$ with R = La [4], Nd [7] for $x \leq 2$ crystallize in a $CaCu_5$ type structure. In case of $RNi_{5-x}Al_x$ with R = Nd, Gd [8], R = Dy [9, 10], R = La [11] systems for $x \geq 2$, the structure changes from $CaCu_5$-type to $HoNi_{2.6}Ga_{2.4}$ type, having also P6/mmm space group.

In this paper we analyze comparatively, the crystal structures and magnetic properties of $RNi_{5-x}Cu_x$ systems with R = La,Nd and $RNi_{5-x}Al_x$ with R = La, Tb, Dy. In addition to magnetic measurements, X-ray photoelectron spectroscopy studies (XPS) and band structure calculations were also performed.

2. Experimental and Computing Method

The samples were prepared in induction or arc furnaces, in purified argon atmosphere. The samples were thermally treated in vacuum at temperatures between 900 and 1000°C during 5 up to 6 days. The X-ray analyses show the presence of only one phase. The composition dependences of the lattice parameters for $DyNi_{5-x}Al_x$ and $NdNi_{5-x}Cu_x$ systems are given in Fig.1.

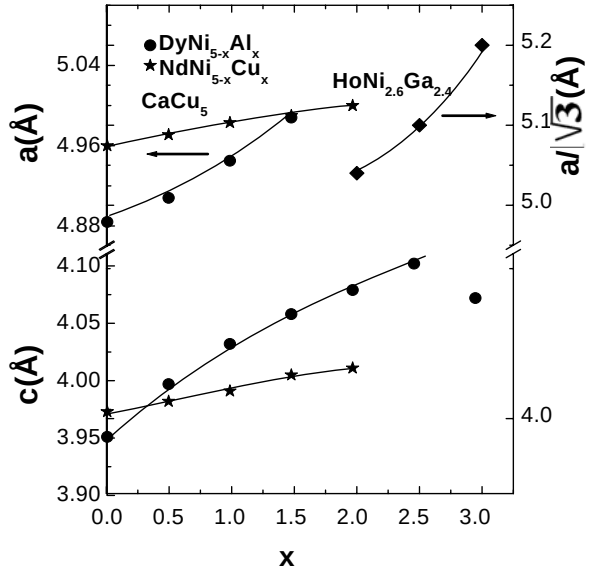

Fig.1 Composition dependences of the lattice parameters for $NdNi_{5-x}Cu_x$ and $DyNi_{5-x}Al_x$ compounds.

For $RNi_{5-x}Cu_x$ with R = La, Nd the presence of $CaCu_5$-type structure was shown for $x \leq 2$. In case of $RNi_{5-x}Al_x$ (R = La, Tb, Dy) having $x \leq 1.5$ also a $CaCu_5$-type structure was observed. For $2 \leq x \leq 3$ the structure changes to a $HoNi_{2.6}Ga_{2.4}$-type. This structure is also hexagonal (P6/mmm space group), but having a larger unit cell than $CaCu_5$-type. The unit cell parameters of the two types of structures are related by $a_{HoNi_{2.6}Ga_{2.4}} = \sqrt{3}a_{CaCu_5}$ and $a_{HoNi_{2.6}Ga_{2.4}} = c_{CaCu_5}$ [8]. In $CaCu_5$-type structure, the aluminum substitution takes place at the 3g site, situated in the z = 1/2 plane which does not contain R atoms. These sites allow greater Ni-Al distances. The total filling of the 3g site by Al is not possible since Ni(2c)-i(3g), Al(3g)-Al(3g) or Ni (3g)-Al(3g) distances are smaller than the sum of metallic radii $r_{Ni}+r_{Al}$ or $r_{Al}+r_{Al}$ [8]. The occurrence of $HoNi_{2.6}Ga_{2.4}$ superstructure induces an increase of the distances Al(3g)-Ni(6k) and Al(3f)-Al(6k) making the possibility to locate aluminum in 3f and 6k sites. In this structure nickel occupies completely 6l sites and aluminum 3f sites. The 6k sites are statistically occupied by Ni and Al.

Magnetic measurements were performed in the temperature range 1.7 – 300 K and fields up to 9 T. The saturation magnetizations, M_s, were determined from magnetization isotherms, according to approach to saturation law $M = M_s (1-b/H)$, by extrapolating the

measured values at $H^{-1} = 0$. By b we denoted the coefficient of magnetic hardness. The paramagnetic contribution of conduction electrons was neglected. The errors introduced by the above assumption ware of the order of 0.1 μ_B/f.u. In the paramagnetic range, the susceptibilities, χ, were determined from their field dependences, according to the relation $\chi = \chi_0 + dM_0H^{-1}$, by extrapolating the measured values to $H^{-1} \rightarrow 0$. By d we denote a presumed magnetic ordered impurity content and M_s is their saturation magnetization. By this method any possible alteration of magnetic susceptibilities, as a result of the presence of small quantities of magnetic ordered phase, is avoided. For all compositions, when exist, the estimated content of magnetic ordered phase, at $T > T_c$, is smaller than 0.1 %.

The XPS measurements were performed by using a PHI 5600 ci Multitechnique system. The spectra were recorded, at room temperature, using monochromatized Al K_α radiation (1486.6 eV). The total resolution, as determined at the Fermi level of a gold foil, was about 0.3-0.4 eV. Binding energies are given with reference to the Fermi level. The $4f_{7/2}$ level of gold was found at 84.0 eV binding energy. The samples were fracturated in the preparation chamber and then moved into the main chamber. All spectra were recorded in a vacuum below $5x10^{-10}$ mbar.

Band structure calculations for $LaNi_{5-x}M_x$ (M = Cu, Al) and $DyNi_{5-x}Al_x$ were carried out by using the ab initio tight binding linear muffin-tin orbitals method in the atomic sphere approximation (TB-LMTO-ASA). The procedure of calculation was described elsewhere [12-14]. In the framework of the local density approximation (LDA), the total electronic potential is the sum of external, Coulomb and exchange–correlation potentials [15]. The functional form of the exchange–correlation energy used in the present work was the free-electron gas parametrization of von Barth and Hedin [16]. Relativistic correlations are included. For $NdNi_{5-x}Cu_x$ and $TbNi_{5-x}Al_x$ systems, band structure calculations were performed by using TB-LMTO within LDA + U approach [17,18]. The LDA + U scheme is based on the Anderson impurity model in mean field (Hartree-Foch) approximation, that analyzes the s and p electrons as noncorrelated, described by an orbital independent potential and d and f electrons are described by an orbital dependent potential [19]. When applied to transition metal and rare-earth compounds, the LDA + U method gives a quantitative improvement compared with LDA for ground state properties such as magnetic moments and interchain exchange parameters [14]. We note that this approach describes well the parallel coupling of Nd and Ni moments. In case of $RNi_{5-x}Cu_x$ systems the Cu atoms, for x=1, was supposed to occupy the 3g sites while for higher Cu concentrations both 2c and 3g positions. In case of $RNi_{5-x}Al_x$, for band structure calculations, the Al was introduced in 3g sites. For $HoNi_{2.6}Ga_{2.8}$ superstructure one Al atom was located in 3f sites and one or two aluminum atoms were distributed in 6k sites.

3. Band Structures

The total density of states as well as the Ni3d bands projected DOS, for some RNi_5 and RNi_4M (R = La, Nd, Tb, Dy and M = Cu or Al) compounds are plotted in Fig.2. In case of RNi_5 compounds the nickel at 0 K, has a magnetic ordered moment in compounds with magnetic rare-earths. The Ni moments are antiparallel aligned to R moments in heavy rare-earths (Tb, Dy) compounds and parallel oriented in light rare-earth (Nd) compounds.

The composition dependences of the magnetic moments at 2c and 3g sites in heavy rare-earth compounds are plotted in Fig.3.

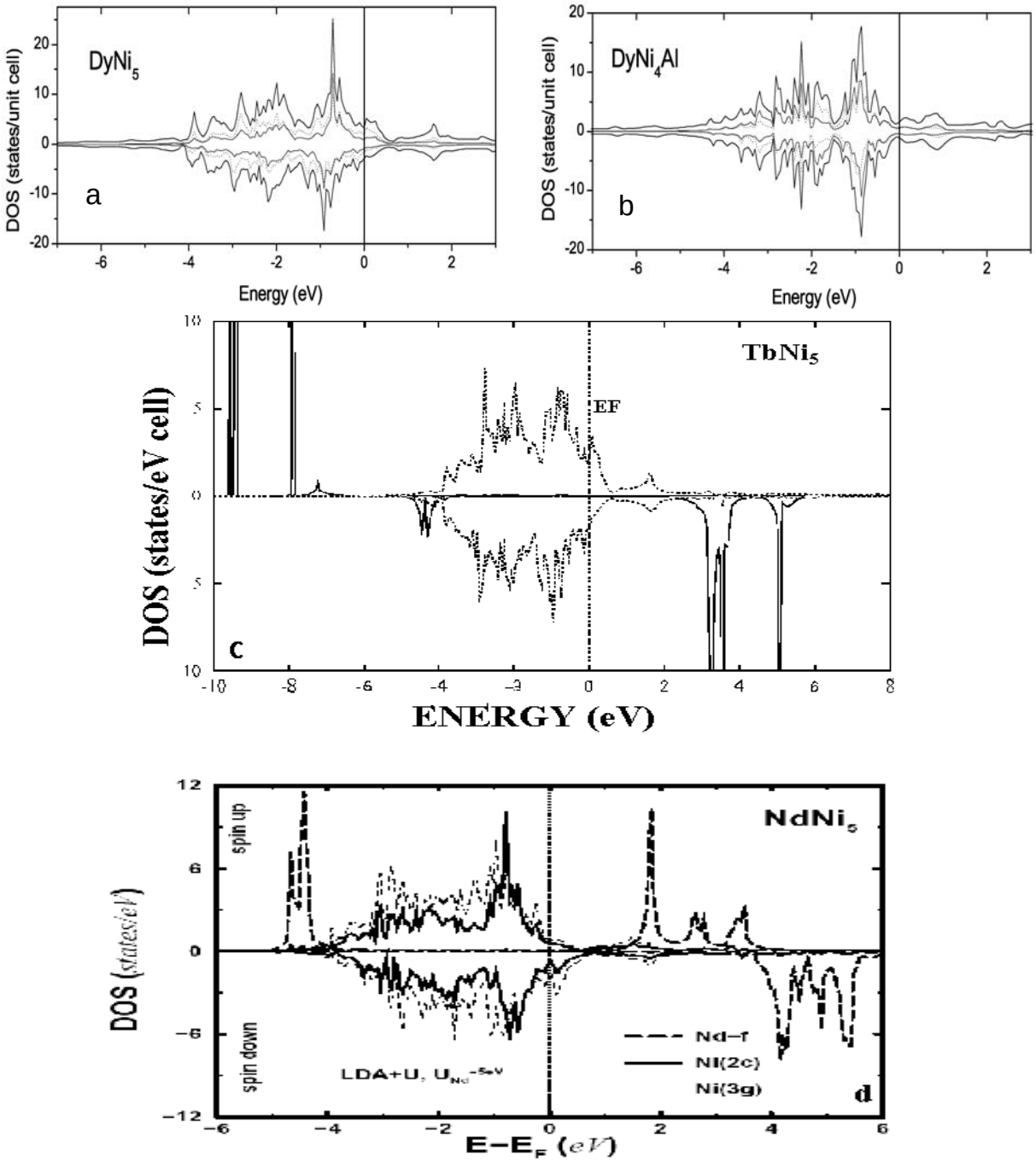

Fig.2 Projected densities of states for $DyNi_5$(a), $DyNi_4Al$(b), $TbNi_5$(c), and $NdNi_5$(d).

The magnetic moments at Ni(3g) sites are higher than those at 2c sites. This behaviour can be attributed to different local environments. The 2c sites in RNi_5 compounds have 6Ni(3g) and 3Ni(2c) atoms as well as 3R ones, while 3g sites have 4Ni(2c), 4Ni(3g) and 4R as nearest neighbours. The strength of the exchange interactions between nickel and magnetic R atoms is more important than between nickel ones, the Ni moments being essentially induced by R atoms. Thus, the exchange splitting of Ni3d(3g) band is greater than

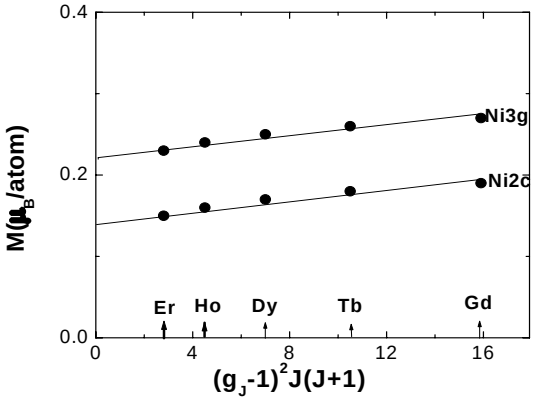

Fig.3 The dependences of Ni(2c) and Ni(3g) moments in RNi_5 compounds as function of De Gennes factor

for Ni3d(2c) one, since of the higher number of R atoms as nearest neighbours. For example, in $NdNi_5$, the exchange splitting of Ni3d(3g) band (0.01 eV) is greater than that at Ni3d(2c) sites (0.0066 eV). We note that the total contribution of Ni atoms to the magnetization is relatively small, particularly in heavy rare-earth compounds.

When replacing nickel by aluminium, the nickel moments, at 0K, decrease rapidly. For example in $DyNi_4Al$, values of 0.03 and 0.04 μ_B were determined at 2c and 3g sites, respectively. Values $M_{Ni}(2c) = 0.02\ \mu_B$ and $M_{Ni}(3g) = 0.03\ \mu_B$ were computed in $TbNi_4Al$ [10]. A somewhat smaller decrease of nickel moments was shown in $NdNi_4Cu$. Values of $\cong 0.06\ \mu_B$ were determined both at 2c and 3g sites. These data suggest a strong hybridization of Ni3d and Al3p bands in aluminium substituted compounds. The variations of the magnetic moments at 2c and 3g sites in Al doped compounds can be correlated with the positions of the center of gravity of various bands [10]. The substitution of one Ni atom by Al in $DyNi_{5-x}Al_x$ decreases the degree of superposition of Ni3d(2c) and Ni3d(3g) bands as evidenced by an increase of the distances between their centers of gravity from $8.5.10^{-3}$ eV to $12.9.10^{-3}$ eV. The difference between the centers of gravity of Ni3d(3g) and Al(3p) bands (0.126 eV) is smaller that between Ni3d(2c) and Al(3p) (0.140 eV) suggesting a higher degree of Ni3d(3g)-Al(3p) bands hybridization. This may account for a higher decrease of the Ni3d(3g) moment (from 0.244 μ_B at x = 0 to 0.04 μ_B (x = 1) than for Ni3d(2c) (from 0.169 μ_B (x = 0) to 0.03 μ_B (x = 1)). The degree of hybridization of Dy5d – Ni3d(3g) bands is not changed for compound with x = 1 as compared to that having x = 0, while that of Dy5d–Ni3d(2c) decreases when replacing Ni by Al. Thus, the exchange interactions decrease as a whole, as evidenced by the diminution of Curie temperature from $T_c = 13$ K (x = 0) to 8 K (x = 1.0). The exchange interactions in R-M (M = Co or Ni) compounds are of 4f-5d-3d type [10]. Using this model we analyze in the following the 5d band polarization.

The R5d band polarizations for RNi_5 and RCo_5 compounds, where R is a heavy rare-earth, as function of De Genness factor, $G = (g_J-1)^2 J(J+1)$ are plotted in Fig.4.

The R5d band polarizations are linearly dependent on the De Gennes factor and can be described by the relation

$$M5d = M_{5d}(0) + \alpha G \qquad (1)$$

The slope α is the same for both series of compounds suggesting that it is characteristic of a given type of structure. We analyzed also this matter in RCo_4B compounds, whose crystal structure is derived from the $CaCu_5$ type. The same slope was evidenced, with $\alpha = 1.4 \times 10^{-2}\ \mu_B$, as in case of RNi_5 and RCo_5 compounds.

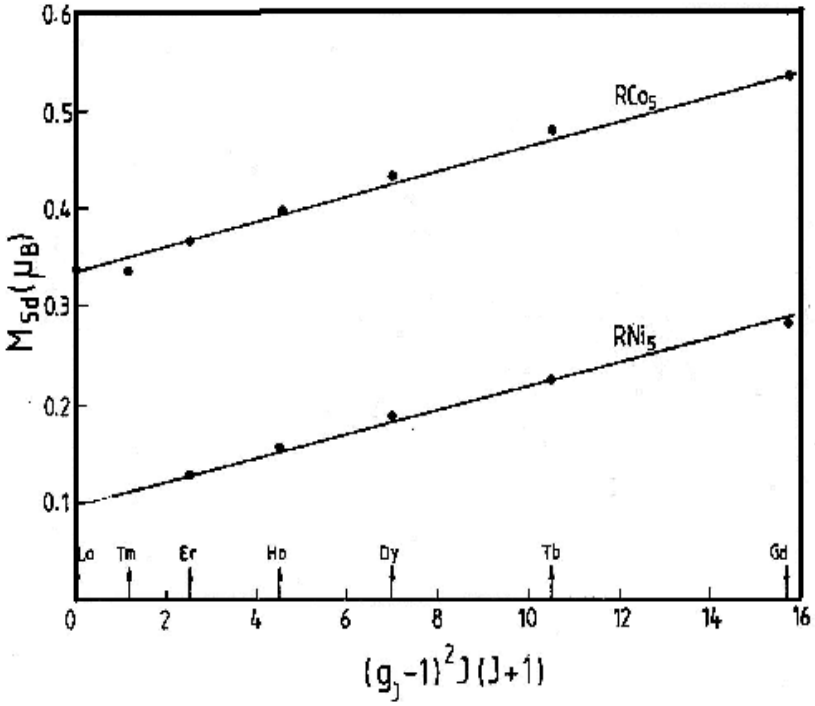

Fig.4 The R5d band polarizations in RNi_5 and RCo_5 compounds.

When increasing the magnetic contributions of transition metals, for a similar rare-earth compound, the R5d band polarization is translated to higher values. Thus, the composition dependence of 5d band polarization, described by relation (1) suggests the presence of two contributions. The first one, αG, is related to the local 4f-5d exchange interactions and seems to be essentially determined by rare-earth moment. The second one, $M_{5d}(0)$, can be attributed to the induced polarization by short range 5d-3d and 5d-5d exchange interactions. The $M_{5d}(0)$ value may be identified by the extrapolation of M_{5d} vs G variation to G = 0. The dominant contribution to $M_{5d}(0)$ is given by the exchange interaction of R5d with neighbouring transition metal atoms. A small contribution is also expected from R5d-R5d exchange interactions, which take place mainly through d_{3z^2-1} orbital with lobes oriented along the **c**-axis. Thus, the short range exchange interactions may be described by the Hamiltonian

$$H = -2\sum_i J_{3d_i\text{-}5d} S_{5d} \sum_{n_i} S_{3d_i,n_i} - 2\, J_{5d-5d} S_{5d} \sum_j S_{5d_j} \qquad (2)$$

We denoted by i the number of 3d atoms situated in the first coordination shell to an R atom, n_c is the number of atoms occupying a given i site and j is the number of R nearest neighbour atoms to a given R site.

The 5d-3d and 5d-5d exchange interactions act as an internal field, H_{exch}, on the 5d band and induce an additional polarization to that given by the local 4f-5d exchange. In the molecular field approximation the exchange field may be written as: $H_{exch} = N_{5d\text{-}3d}M_{3d} + N_{5d\text{-}5d}M_{5d}$, where $N_{5d\text{-}3d}$ and $N_{5d\text{-}5d}$ are the molecular field coefficients describing the R5d-M3d and R5d-R5d exchange interactions, respectively. In RCo_5 compounds, the contribution of second term in (2) may be neglected since $S_{3d} \gg S_{5d}$. For RNi_5 compounds the 5d band polarization is of the order of Ni3d moments, and consequently the last term in (2) cannot be neglected. In this case a reasonable approximation is $N_{5d\text{-}3d} \cong N_{5d\text{-}5d}$. As a result, the exchange field is proportional to total d magnetization, $M_d = M_{3d} + M_{5d}$, namely $H_{exch} = \xi M_d$. Previously [20], we showed that the induced 3d band polarization in rare-earth-transition

metal compounds is proportional to the exchange field, $\Delta M_d \propto \Delta H_{exch}$. Consequently, we have $M_{5d}(0) = \gamma M_d$. According to the above relation, as well as the Hamiltonian (2), the polarization is proportional to the $\sum n_k M_k$, where n_k is number of R and M atoms situated in first coordination shell having M_k magnetic moments. The $M_{5d}(0)$ values are plotted in Fig. 5 as function of $\sum n_k M_k$. In addition to data obtained for RNi_5 and RCo_5-based compounds, the 5d polarization for R(1a) and R(1b) sites in RCo_4B compounds is also given. As seen in Fig. 5, there is a linear dependence of $M_{5d}(0)$ on $\sum n_k M_k$. The slope is $\gamma = 0.04$. The same value was obtained for the ratio $M_{5d}(0)/M_d$ in RNi_5 and RCo_5 compounds. In the above discussion we considered the contributions to 5d band polarization as additive. In reality these values are reciprocal influenced and can be determined self consistently. The errors introduced by this approximation were estimated to be smaller than 8 %.

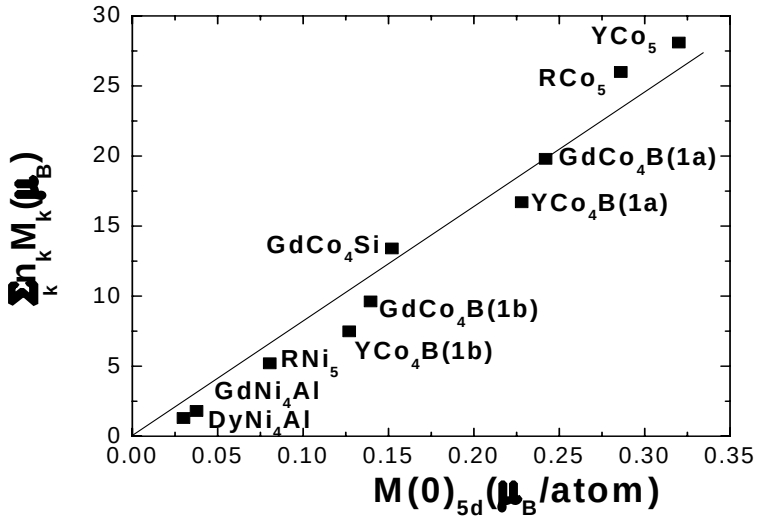

Fig.5: The $M_{5d}(0)$ contributions to 5d band polarization as function of $\sum n_k M_k$, the d magnetic moments of atoms situated in first coordination shell.

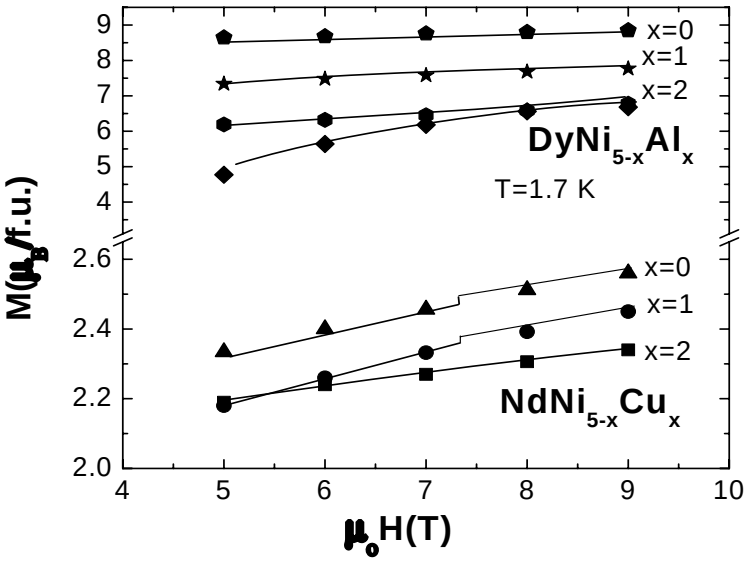

Fig.6 Magnetization isotherms, at 1.7 K, for $NdNi_{5-x}Cu_x$ and $DyNi_{5-x}Al_x$ compounds.

4. Magnetic Data

Representative magnetization isotherms, at 1.7K, for $DyNi_{5-x}Al_x$ and $NdNi_{5-x}Cu_x$ compounds are plotted in Fig.6. The saturation is more hardly to be obtained for higher aluminum substitution in $DyNi_{5-x}Al_x$ compounds. In addition, the magnetizations decrease when increasing the Al content. This behaviour is different from that expected considering an antiparallel alignment of Dy and Ni moments. As the Ni moments decrease, as shown from band structure calculations, the saturation magnetization must increase. Analyzing also the magnetization isotherms for sample with x = 2,3 we attribute the above unexpected behaviour to a micromagnetic type contribution superposed on an essentially ferromagnetic type ordering. We note that for compounds with $x \leq 1$, the experimentally determined magnetizations are close to those obtained from band structure calculations. The Curie temperatures, T_c, decrease form 13K (x=0) to 8K (x=1) and 5K (x=2). High decrease of T_c values was also shown in $TbNi_{5-x}Al_x$ system. Values T_c = 23 (x=0), 20K (x=1) and 11K (x=2) were evidenced [21].

The magnetization isotherms for $NdNi_{5-x}Cu_x$ system, at 1.7 K, show for x = 0, the presence of a relatively high anisotropy. The M = f (H) curves saturate at lower field as the copper content increases. Thus, the coefficient of magnetic hardness decreases from a = 0.92 (x=0) to 0.32 (x=1) and 0.03 for x=1.5. These data suggest that Cu substitutes also nickel sites having high anisotropy. The largest orbital moment was seen in cobalt isomorphous compounds, at 2c site, which can be connected with a higher contribution to the anisotropy. This shows that a fraction of copper is located also in 2c sites. The saturation magnetizations experimentally determined are by 0.2-0.3 μ_B/f.u. smaller than those obtained from band structure calculations. The magnetization isotherms for compounds with x=0 and 0.5 show small discontinuities between 7 and 8 T. This behaviour cannot be seen for higher copper content. This may be correlated with a possible itinerant metamagnetic transition at some Ni sites. The Curie temperature of $NdNi_5$ is T_c = 9 K and decreases at 6 K for x = 1.0.

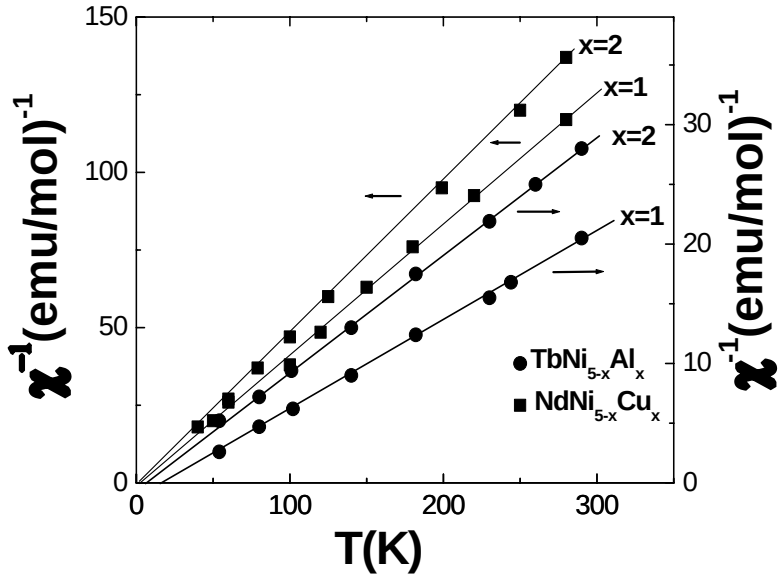

Fig.7. Thermal variations of reciprocal susceptibilities for $TbNi_{5-x}Al_x$ and $NdNi_{5-x}Cu_x$ compounds with x = 1 and 2

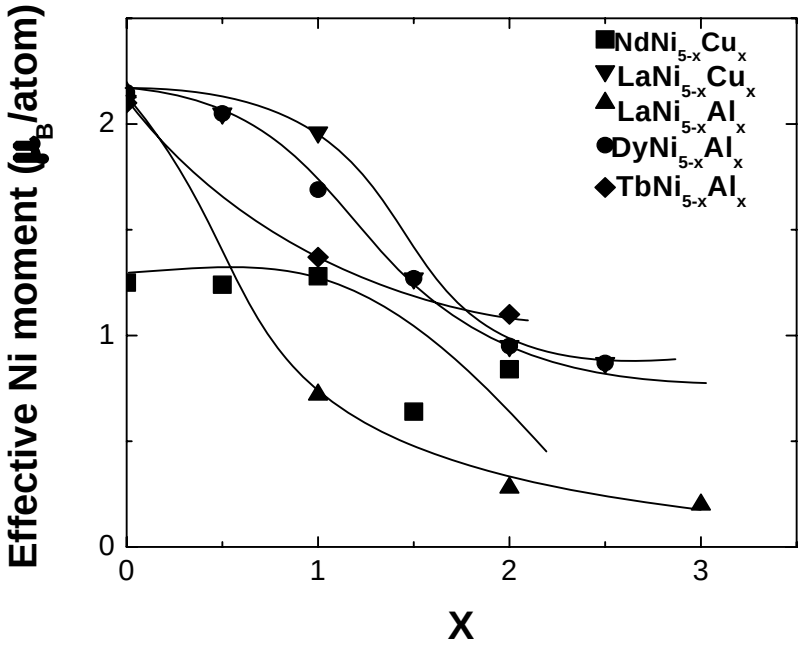

Fig.8 Composition dependences of the effective nickel moments.

The thermal variations of reciprocal susceptibilities for some representative compounds with magnetic rare earths are plotted in Fig 7. Curie-Weiss type dependences are shown, as described by the relation

$$\chi = \chi_0 + C(T-\theta)^{-1} \qquad (3)$$

We denoted by C the Curie constant, θ is the paramagnetic Curie temperature and χ_0 a Pauli type term. In the above systems, the χ_0 contribution can be neglected.

The Curie constants are somewhat higher than those of free R^{3+} ions. Consequently, a contribution from nickel to C values is also suggested. According to addition law of magnetic susceptibilities and supposing that the effective moments of R ions are given by free R^{3+} values we determined the contributions of nickel to the Curie constants and the effective nickel moments, respectively. These values are plotted in Fig.8. The effective nickel moments in doped aluminium systems decrease more rapidly than in case of cooper ones, suggesting a strong hybridization of Ni3d and Al3d bands.

The magnetic behaviour of $LaNi_{5-x}M_x$ with M = Cu or Al were also studied – Fig.9 [4,11].

The magnetic susceptibilities increase up to a characteristic temperature, T_{max}. The T_{max} values are shifted to lower temperatures when increasing copper or aluminum content. Above a characteristic temperature, T^*, the reciprocal susceptibilities follow a Curie-Weiss type dependence, described by relation (3). The χ_0 contribution is important in Al substituted compounds and can be connected with the strong Ni3d-Al3p band hybridization. The Pauli type contributions increase from 1.0×10^{-4} emu/f.u. (x = 1) to 1.80×10^{-4} emu/f.u. (x = 2) and 1.85×10^{-4} emu/f.u. at x = 3.

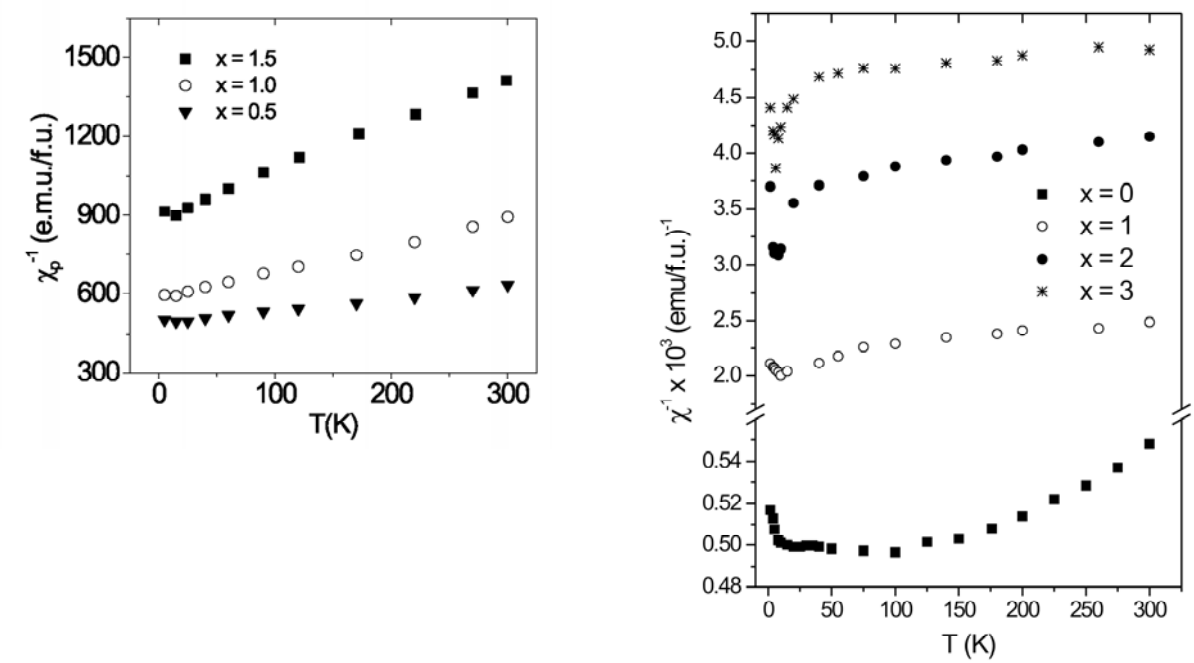

Fig.9 Thermal variations of reciprocal susceptibilities for $LaNi_{5-x}Cu_x$ (a) and $LaNi_{5-x}Al_x$ (b) compounds.

For copper doped systems the χ_0 values are of the order of 10^{-5} emu/f.u. and can be neglected as compared to second term of relation (3). The effective nickel moments determined from Curie constants are plotted in Fig. 8. These follow the same trend as for compounds with magnetic rare-earths. A stronger decrease of M_{eff}(Ni) in aluminium compounds was shown. The paramagnetic Curie temperatures are negative and decrease in absolute magnitude as the Al or Cu content increases.

The calculated magnetic susceptibilities from band structures, at 0 K, and those experimentally determined, at 1.7 K are plotted in Fig. 10. There is a good agreement between two sets of data. A higher decrease was shown for aluminium substituted samples than for copper doped ones.

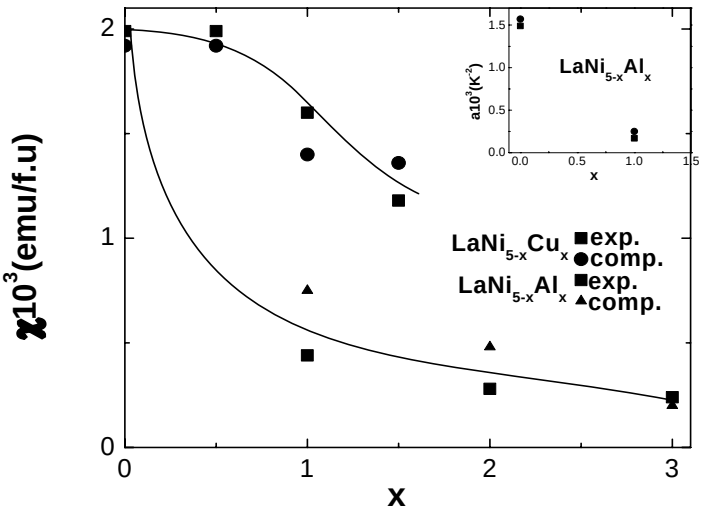

Fig.10. Composition dependences of the susceptibilities, determined at 1.7 K, in $LaNi_{5-x}Cu_x$ and $LaNi_{5-x}Al_x$ and those obtained from band structure calculations. In the inset the determined and computed values for $LaNi_{5-x}Al_x$ with x = 0 and 1.0 are given.

In the low temperature range (T≤10 K), the magnetic susceptibilities follow a dependence described by the relation – Fig. 11:

$$\chi = \chi_0(1 + aT^2) \tag{4}$$

with

$$a = \frac{\pi^2}{6}\left[\left(2\frac{N''(E_F)}{N(E_F)} - 1.2\left(\frac{N'(E_F)}{N(E_F)}\right)^2\right)\right]\cdot s^2 \tag{5}$$

as determined considering the paramagnon model [22].

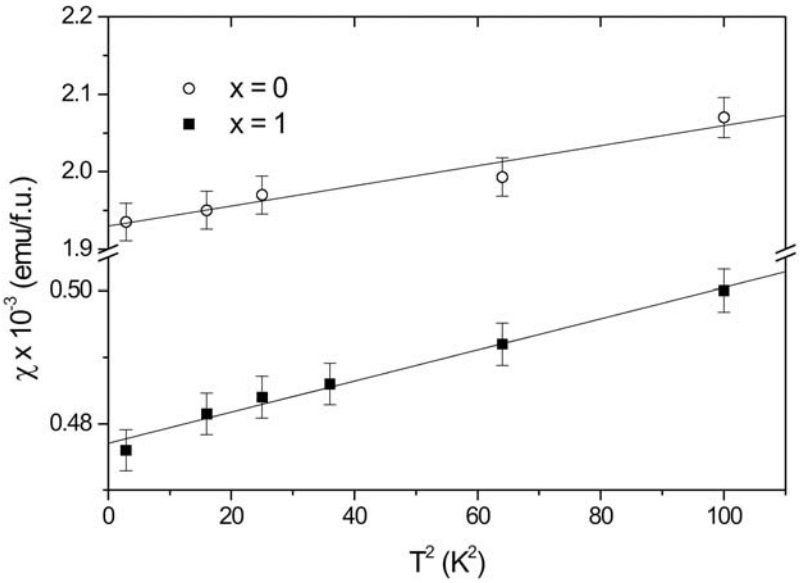

Fig.11 Temperature dependences of the magnetic susceptibilities for $LaNi_{5-x}Al_x$ system with x=0 and 1, at T≤10 K.

We denoted by s the Stoner enhancement factor and $N(E_F)$, $N'(E_F)$, $N''(E_F)$ are the density of states at the Fermi level and their first and second derivatives, respectively. We selected a symmetric energy interval around the self-consistent value of the Fermi level, and we used a mean square interpolation scheme in order to analytically evaluate the energy dependence of the density of states. This approach allowed us to evaluate the first and the second derivative of the DOS at the Fermi level. The values a, thus determined, according to relation (5), agree reasonably with those experimentally determined – inset Fig.11.

5. XPS Measurements

The Nd3d core level spectra in $NdNi_{5-x}Cu_x$ are plotted in Fig. 12a. The $Nd3d_{3/2}$ line is situated at 1003.6 ± 0.2 eV and that of $Nd3d_{5/2}$ at 981.2 ± 0.2 eV. The apparently small shift to higher binding energy (≅ 0.4 eV) as compared to pure neodymium lines was attributed to the presence of small Nd_2O_3 content. The Dy4d core level spectra in $DyNi_{5-x}Al_x$ compounds were decomposed in four lines located at 152.3 ± 0.2 eV, 153.6 ± 0.2 eV, 155.0 ± 0.2 eV and 157.0 ± 0.2 eV – Fig. 12b. These are similar as those observed in Dy metal. We conclude that there are no changes in the positions of Nd3d and Dy4d core lines, as compared to pure metals, in both series of compounds.

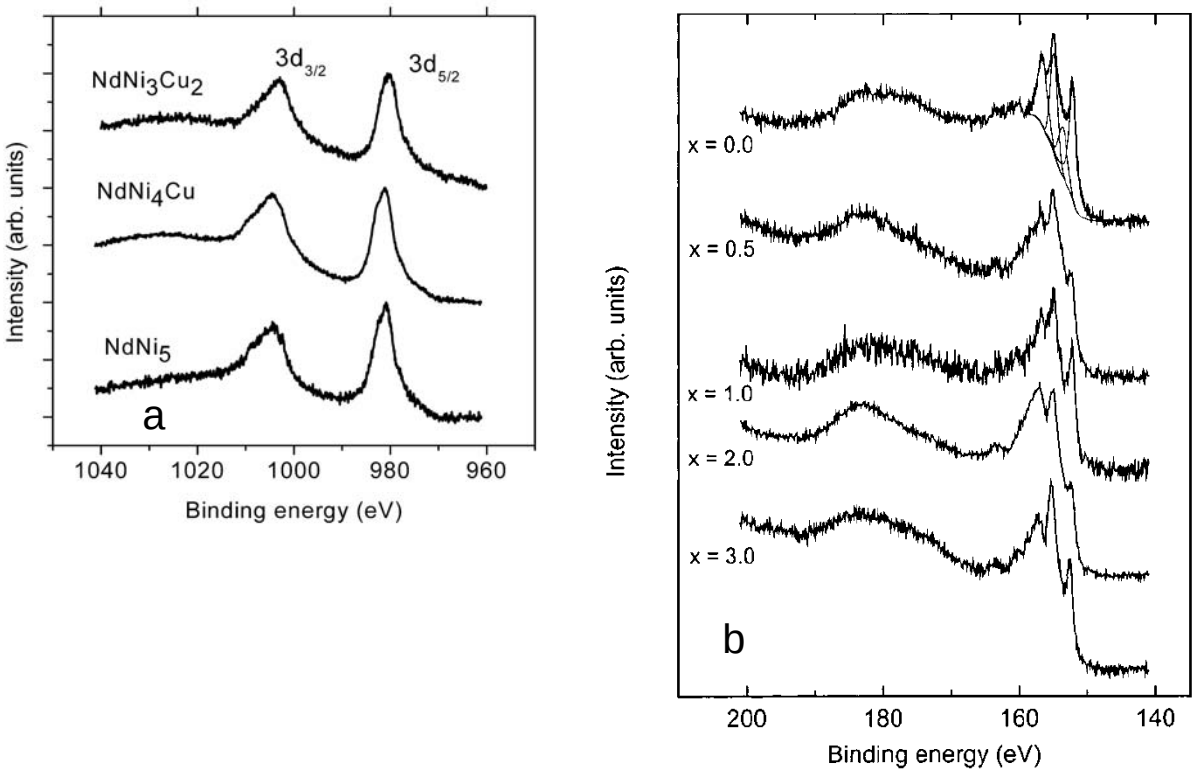

Fig.12. The Nd3d (a) and Dy4d (b) XPS spectra in $NdNi_{5-x}Cu_x$(a) and $DyNi_{5-x}Al_x$(b) compounds.

The $Ni2p_{3/2}$ and $Ni2p_{1/2}$ core level lines for some representative compounds are plotted in Fig.13. For comparison, the Ni2p spectrum of pure nickel is also given. The spectra were decomposed, as for pure nickel, considering the main lines and satellites. For example in $NdNi_{5-x}Cu_x$ system, the positions of the $2p_{3/2}$ and $2p_{1/2}$ line are situated at 852.5 ± 0.1 eV and 826.9 ± 0.1 eV, respectively and do not change with composition. These lines are located at the same binding energies as for pure nickel (852.7 ± 0.1 eV and 869.97 ± 0.1 eV, respectively). The 6 eV satellite is located at 858.5 ± 0.1 eV in $NdNi_{5-x}Cu_x$ system. The same behaviour was shown in other copper substituted compounds. Thus, the positions of the main and satellite lines are not changed with composition, in copper substituted system. A slight shift to higher binding energies was shown when Ni is replaced by Al. Thus, in $DyNi_{5-x}Al_x$ compounds the shifts of the Ni2p lines are of 0.1 eV (x = 0.5), 0.25 eV (x = 1.0), 0.3 eV (x = 2.0) and 0.6 eV (x = 3.0). There is also a more pronounced decrease of the Ni6 eV satellite intensities, when increasing Al content, than in Cu system. These features can be correlated with changes in nickel band structures, as a result of filling 3d band due to hybridization effects.

The Cu2p core lines, for $NdNi_{5-x}Cu_x$ system, are plotted in Fig. 14. The binding energies for $Cu2p_{3/2}$ states are situated at 932.5 ± 0.1 eV [7]. This value is close to that characteristic of pure copper located at 932.7 eV [23]. The $2p_{1/2}$ core lines for all compositions are situated at 952.3 eV, close to the value characteristic of pure copper (952.5 eV). Similar behaviour was shown in $LaNi_{5-x}Cu_x$ system. Taking into account that for Cu core level spectra, there are no satellite structures and in addition the lines are narrow, we conclude that the electronic configuration of copper is $3d^{10}$ (in atomic notation).

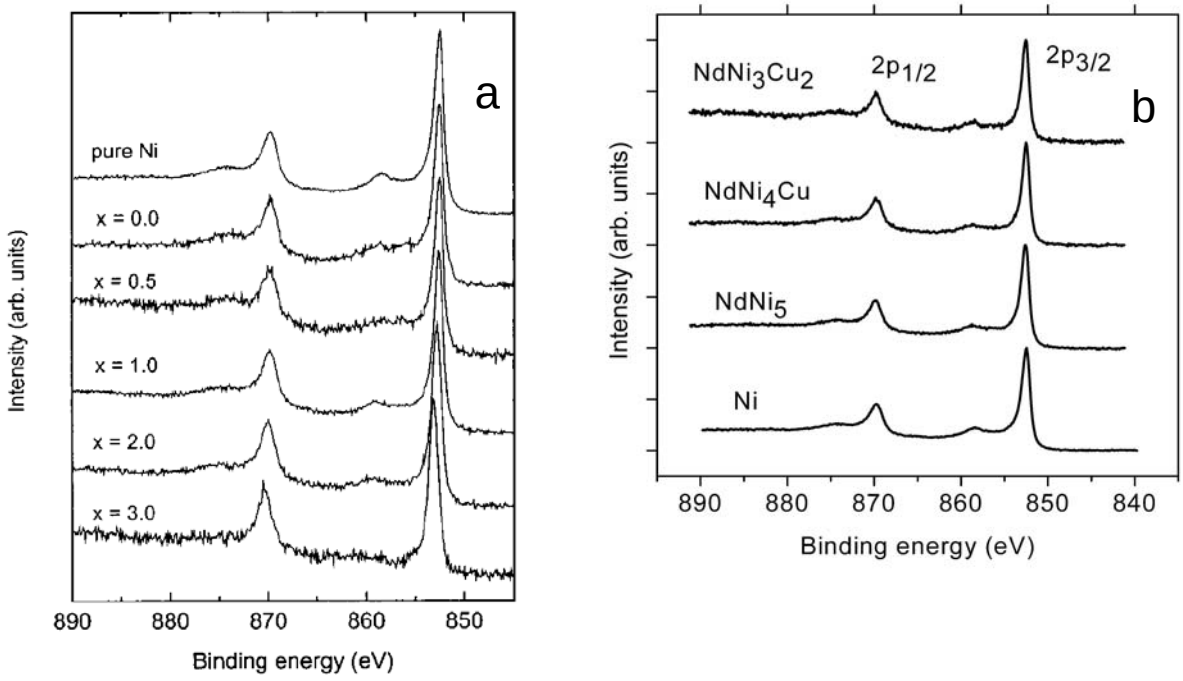

Fig.13. The $Ni2p_{3/2}$ and $2p_{1/2}$ core lines for some $DyNi_{5-x}Al_x$ (a), $NdNi_{5-x}Cu_x$ (b) and $LaNi_{5-x}Cu_x$ (c) representative compounds.

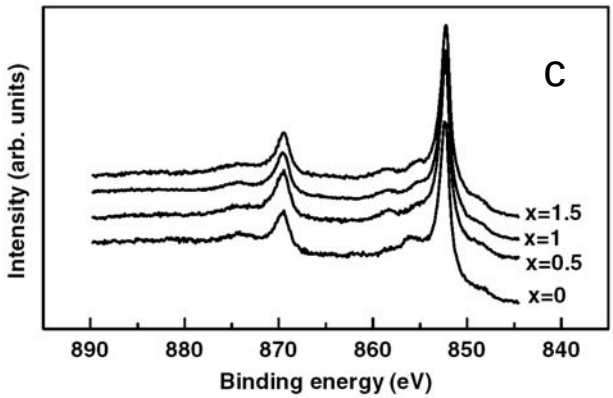

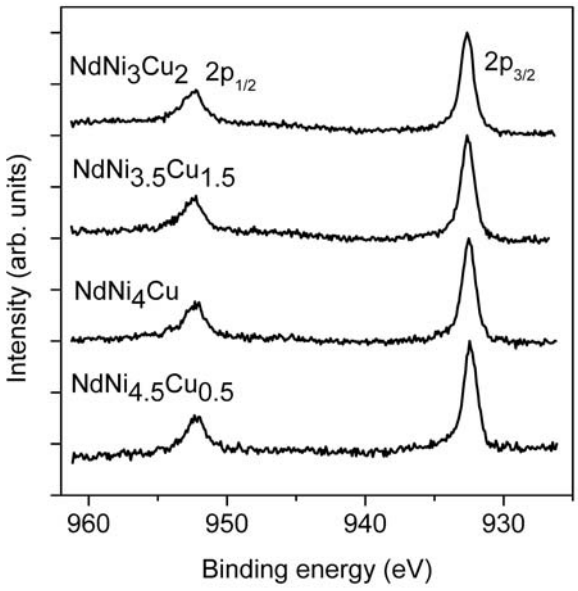

Fig.14. Cu2p core lines in $NdNi_{5-x}Cu_x$ system.

The XPS valence bands of $LaNi_{5-x}M_x$ with M = Al and Cu are plotted in Fig. 15, together with that of pure nickel.

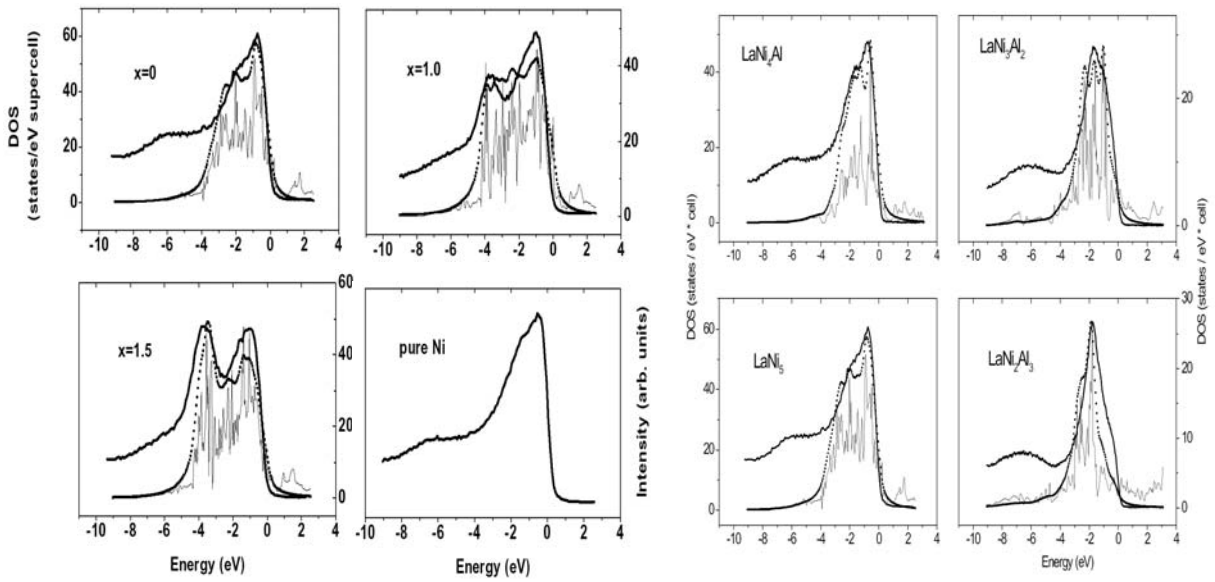

a b

Fig.15. Comparison of the measured XPS valence bands (thick solid line), the calculated total DOS (solid line) and the convoluted DOS (with Lorentzian of half-width 0.4 eV and taking into account appropriate cross-sections for partial bands with different l-symmetry; dashed line) for $LaNi_{5-x}Cu_x$ (a) and $LaNi_{5-x}Al_x$ (b) series.

There is a similarity of the Ni3d bands for pure Ni with those for $LaNi_5$. This fact evidences that the valence band of $LaNi_5$ is mainly derived from Ni d states. There is also present the 6.0 eV Ni satellite. The intensity of satellites decreases when increasing Al content. In addition, the density of states at the Fermi level is diminished as compared with that of pure nickel and the maxima of the valence bands are shifted to higher binding energy. The positions of the maxima, as compared to Fermi level, are 0.59 eV for pure Ni, 0.67 eV in $LaNi_5$ and 0.80 eV in $LaNi_4Al$. In $LaNi_3Al_2$ the shift is by 1.60 eV and in $LaNi_2Al_3$ by 1.74 eV. The states at the Fermi level have mainly d character in $LaNi_5$. On alloying with aluminium, the s-p contribution to the DOS, at the Fermi level increases. In $DyNi_{5-x}Al_x$ the maxima in the valence band spectra are located at 0.65 eV (x = 0), 0.72 eV (x = 0.5) and 0.77 eV (x = 1.0) [10] near the same positions as shown in $LaNi_{5-x}Al_x$. Due to complexity of the spectra, the 6 eV satellite cannot be observed since of superposition with Dy bands.

The computed density of states in $LaNi_{5-x}Al_x$ describes rather well the general features of experimental spectra-Fig.15 [11]. The orbital-projected partial densities of states were multiplied with approximate cross-sections for 1486.6 eV incident radiation and their sum was then convoluted with Lorentzians of half-width 0.4 eV. There are also some differences between the two sets of spectra. These can be attributed to the fact that band structures were computed at 0 K and those obtained by XPS were recorded at room temperature. In addition, the correlation effects were not considered in computing the density of states. Also, the inelastic scattering background present in the XPS spectra was not substracted.

Alloying with Cu in $LaNi_{5-x}Cu_x$ system does not induce visible changes in the Ni d-band – Fig.15. A rather independent Cu d-band is formed at around 3.3 eV binding energy. By increasing Cu content, the relative intensity of Cu d band is increased. The width of Cu

line is not changed when increasing the Cu content. These Cu states are probably completely filled with electrons.

The XPS valence bands of $NdNi_{5-x}Cu_x$ samples are plotted in Fig. 16.

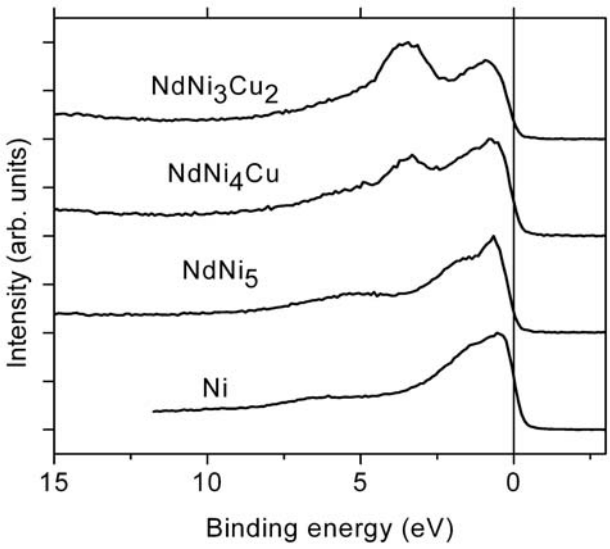

Fig.16. XPS valence band spectra of some $NdNi_{5-x}Cu_x$ compounds.

The 4f orbitals of Nd keep their localized character and therefore the XPS spectra show multiplet structures. These correspond to transitions between the ground state of configuration $4f^n$ and the accessible final states $4f^{n-1}$. The spectrum can be considered as a finger of the number of 4f electrons in the initial state. Thus, the XPS valence band spectrum of neodymium [24] evidences the presence of Nd4f contribution to the valence band at $\cong$ 4.65 eV binding energy corresponding to $^3H_4$ state and those of Nd5d states at about 1 eV binding energy, the latter being spread up to Fermi level. In the valence band spectra of $NdNi_{5-x}Cu_x$, the the Nd lines are rather difficult to be observed since of their low intensity as well as due to the superposition with copper lines. Due to 5d-3d hybridization, the shape of nickel spectrum in $NdNi_5$ is somewhat modified around the Fermi level, as compared to pure Ni. Thus, although the valence band spectrum is similar to that of pure nickel, the density of states at the Fermi level is diminished. In addition, the valence band of Ni in $NdNi_5$ is shifted to higher energy. This may be correlated with an increase of d-state occupancies. When substituting Ni by Cu, rather independent Cu d band is formed at around 3.3 eV binding energy. As in case of $LaNi_{5-x}Cu_x$ system, the relative intensities of Cu d bands increase but their positions and the linewidths are not changed when composition is modified.

6. Magnetic Behaviour of Nickel and Rare-Earths

The XPS measurements, at room temperature, on $DyNi_{5-x}Al_x$ and $NdNi_{5-x}Cu_x$ systems on Nd4f and Dy4f show that the crystal field is well shielded by the valence electrons and is small compared with the separation of the multiplet states. This is in agreement with the results of magnetic measurements, which show that the rare-earth moments are close to the g_JJ values.

The exchange interactions in compounds with magnetic rare-earths can be well described by the Campbell model [25] which considers the 4f-5d-3d exchange interactions. The R4f electrons polarize the R5d band through local exchange interactions. The induced 5d polarization in heavy rare-earth compounds is parallel to the 4f moments. There are also short

range exchange interactions of 5d-3d and 5d-5d types which induced additional 5d band polarization.

The band structure calculations show that Ni moments at 0 K decrease very fast in the composition range $0 \le x \le 1$ and are near nil for higher Al or Cu substitutions. This behaviour can be attributed to hybridization effects and diminution of electron correlations between d electrons. There is a linear dependence of nickel moments at 2c and 3g sites on the exchange splitting of their 3d band. The extrapolation to nil nickel moment suggests a critical field for the appearance of a nickel moment of $\mu_0 H_{exch} = 30 - 40$ T.

In the paramagnetic range, for all studied composition, an effective nickel moment, $M_{eff}(Ni)$, is present. The $M_{eff}(Ni)$ values decrease when increasing the content of Cu or Al. The presence of unoccupied Ni3d states is also suggested by the XPS measurements, at room temperature. The Ni 6 eV satellite lines were shown in the whole composition range although their intensities decrease when increasing Cu or Al content.

The $LaNi_{5-x}M_x$ with M = Cu or Al compounds show an interesting behaviour. The magnetic susceptibilities, χ increase up to a temperature T_{max}. In low temperature range, $T \le 10$ K, a T^2 dependence of χ values was shown. Above a characteristic temperature, T^*, a Curie-Weiss behaviour was evidenced. Thus, the nickel, at 0 K, has a weak moment or shows an enhanced magnetic susceptibility. In the high temperature range, the linear χ^{-1}vsT dependences suggest the presence of localized nickel moments. The above behaviour may be analyzed in models, which take into account the electron correlations effects in d-band, as spin fluctuation model [6] or dynamical mean field theory [26]. These models reconcile the dual character of electron, which as particle requires a real space description and as a wave, a momentum space description. The spin fluctuation model considers the balance between the frequencies of longitudinal spin fluctuation, which are determined by their lifetime and of transverse fluctuations, which are of thermal origin. These effects lead to the concept of temperature induced moment. For a weak ferromagnet as Ni in $RNi_{5-x}M_x$ (R = Nd, Tb, Dy) with $x \le 1$ or an exchange enhanced paramagnet as for compositions $x \ge 2$ or Ni in $LaNi_{5-x}M_x$ (M = Cu, Al), systems, the wave number dependent susceptibility, χ_q, has a large enhancement due to electron-electron interaction for small q-values. The χ_q shows a significant temperature dependence only for q values close to zero. The average amplitude of spin fluctuations $\left\langle S_{loc}^2 \right\rangle = 3k_B T \sum \chi_q$ increases with temperature and reaches an upper limit at a temperature T^*. For $T > T^*$, a Curie-Weiss behaviour is predicted, similar as in systems having local moments. The moments are localized in q-space. If the spin fluctuations are saturated, feature, which characterizes the systems having high exchange enhancement factors or are weak ferromagnets, the effective moments reflect the electronic configuration of the given 3d ion. The effective nickel moments in RNi_5 are somewhat lower ($\cong 2.15\ \mu_B$) than the value expected for Ni^{2+} ion ($2.82\ \mu_B$). This decrease may be attributed to the diminution of electron correlations due to 3d-5d hybridization. We note that in spin fluctuation model, the effective Ni moments and those obtained at 0 K are not correlated [6].

The magnetic behaviour of nickel in the studied compounds, may be also analyzed in the dynamical mean field theory DMFT [26] combined with the standard LDA band calculations (LDA + DMFT) [27]. In a strongly correlated system, leading Curie-Weiss behaviour, at high temperatures, is predicted. For an itinerant electron system, the time dependence of the correlation function results in a temperature dependence of $\left\langle S_{loc}^2 \right\rangle$. Fluctuating moments and atomic-like configurations are large at short time. The moments are reduced at larger time scales, corresponding to a more band like less correlated electronic

structure near the Fermi level. By using a numerically exact quantum scheme, in the LDA + DMFT, it was possible to reproduce the 6 eV satellite in DOS spectrum of nickel at $T = 0.9T_c$. This satellite was shown to have substantially more spin-up contribution. The diminution of the 6 eV satellite intensity, as evidenced by XPS measurements, in samples where Ni was substituted by Al or Cu is in agreement with partial filling of Ni3d band due to hybridization effects. The above data are also in agreement with magnetic measurements which show a decrease of the effective nickel moments when increasing the content of substituting elements.

7. Conclusions

The $RNi_{5-x}Cu_x$ series with R = La, Nd form solid solutions having $CaCu_5$ type structure in the composition range $x \leq 2.5$. In $RNi_{5-x}Al_x$ systems with R = La, Tb, Dy, the structure changes to $HoNi_{2.6}Ga_{2.4}$ type for $x \geq 2$.

Band structure calculations on RNi_5 compounds with magnetic rare-earths show the presence of nickel ordered magnetic moments at both 2c and 3g sites. The nickel moments are antiparallel aligned to rare-earth for R = Tb, Dy and parallel oriented for R = Nd. The values of the nickel moments were correlated with their local environments. The nickel moments decrease when replacing Ni by Cu or Al and are practically nil for $x \geq 2$. Above the magnetic ordering temperatures, Curie-Weiss dependences were shown. The Curie constants are higher than those of free R^{3+} ions suggesting the presence of nickel contributions. The effective nickel moments decrease when increasing Al or Cu content, but have finite values in the whole studied composition range.

The $LaNi_{5-x}Cu_x$ and $LaNi_{5-x}Al_x$ compounds, where La is not magnetic, show at low temperatures ($T \leq 10$ K), a T^2 dependence of the magnetic susceptibilities χ. The χ values obtained from band structure calculations agree with those experimentally determined at 1.7 K. Above a characteristic temperature T^*, a Curie-type contribution is evidenced. The effective nickel moments follow the same composition dependence as that evidenced in compounds with magnetic rare-earths. The XPS studies, at room temperature, show in all cases the presence of 6 eV satellite suggesting that there are unoccupied Ni d states, the intensity of the satellite decreasing when increasing the content of substituting elements. The magnetic behaviour of nickel is described in models, which take into account the electron correlation effects in d bands as spin fluctuation model or dynamical mean field theory.

References

[1] E. Burzo, A. Chelbowski and H.R. Kirchmayr, Landolt Börnstein Handbuch, vol. III/19d2, Springer Verlag, (1990)
[2] D. Gignoux, D. Givord and A. del Moral, Solid State Commun. 19, 891 (1976)
[3] E. Burzo, L. Chioncel and I. Costina, Mat. Sci. Forum 373-376, 669 (2001)
[4] E. Burzo, S.G. Chiuzbaian, L. Chioncel and M. Neumann, J. Phys.: Condens. Matter 12, 5897 (2000)
[5] E. Burzo, V. Pop and I. Costina, J. Magn. Magn. Mater. 157-158, 615 (1996)
[6] T. Moriya, J. Magn. Magn. Mater. 100,201 (1991)
[7] E. Burzo, T. Crainic, M. Neumann, L. Chioncel and C. Lazar, J. Magn. Magn. Mater. (in press)
[8] J.L. Bobet, S. Pechev, B. Chevalier and B. Darriet, J. Alloys Compounds 267,136 (1998)
[9] S. Sorgic, A. Dasner and Z. Blazine, J. Phys.: Condens. Matter. 7, 7209 (1995)

[10] E. Burzo, S.G. Chiuzbaian, M. Neumann, M. Valeanu, L. Chioncel and I. Creanga, J. Appl. Phys. 92,7362 (2002)
[11] E. Burzo, S.G. Chiuzbaian, M. Neumann and L. Chioncel, J. Phys.: Condens. Matter. 14, 8057 (2002)
[12] O.K. Anderson, Phys. Rev. B12, 3060 (1975)
[13] O.K. Anderson and O. Jepsen, Phys. Rev. B53, 2571 (1984)
[14] O.K. Anderson, O. Jepsen, and D. Glötzel, Highlights of Condensed Matter. Theory, Ed. F. Bassani, F. Fumi and M.P. Tossi, New York, North-Holland, 1985
[15] R.O. Jones and O. Gunnarson, Rev. Mod. Phys. 61, 689 (1989)
[16] U. von Barth and L. Hedin, J. Phys. C.: Solid State Phys. 5, 1629 (1972)
[17] V.I. Anisimov, J. Zaanen and O.K. Anderson, Phys. Rev. B44, 943 (1991); A.I. Lichtenstein, J. Zaanen and V.I. Anisimov, Phys. Rev. B52, R 5467 (1995)
[18] V.I. Anisimov, I.V. Solovyev, M.A. Korotkin, T.H. Cyzyk and G.A. Sawatzky, Phys. Rev. B48, 16929 (1993)
[19] V.I. Anisimov, F. Aryasetiavan and A.I. Lichtenstein, J. Phys.: Condens. Matter. 9, 767 (1997)
[20] E. Burzo, Solid State Commun. 14, 1295 (1974)
[21] E. Burzo, A. Takacs, M. Neumann and L. Chioncel, Phys. Stat. Solidi (in press)
[22] M.T. Béal-Monod, Physica B 139-140, 1837 (1982)
[23] B. Vincent Crist, Handbook of Monochromatic XPS Spectra, vol. I, XPS International Inc., 1999
[24] J.K. Lang, Y. Bauer and P.A. Cox, J. Phys. F.: Metal Phys. 11, 121 (1981)
[25] I.A. Campbell, J. Phys. F.: Metal Phys. 2, L149 (1972)
[26] A. Georges, G. Kothar, W. Krauth and M.J. Rosenberg, Rev. Mod. Phys. 68, 13 (1996)
[27] A.I. Lichenstein, M.I. Katsnelson and G. Kothar, Phys. Rev. Letters 87, 672205 (2001)